Title
Directional excitation without breaking reciprocity

Journal
New Journal of Physics, 18(9)

ISSN
1367-2630

Authors
Ramezani, Hamidreza
Dubois, Marc
Wang, Yuan
et al.

Publication Date
2016-09-01

DOI
10.1088/1367-2630/18/9/095001

Peer reviewed

PAPER • OPEN ACCESS

Directional excitation without breaking reciprocity

New Journal of Physics
The open access journal at the forefront of physics

Deutsche Physikalische Gesellschaft DPG
IOP Institute of Physics

Published in partnership with: Deutsche Physikalische Gesellschaft and the Institute of Physics

OPEN ACCESS

RECEIVED
23 February 2016

REVISED
20 July 2016

ACCEPTED FOR PUBLICATION
1 August 2016

PUBLISHED
2 September 2016

PAPER

Directional excitation without breaking reciprocity

Hamidreza Ramezani[1,2,5], Marc Dubois[1,5], Yuan Wang[1], Y Ron Shen[3,4] and Xiang Zhang[1,4]

[1] NSF Nanoscale Science and Engineering Center, University of California, Berkeley, CA 94720, USA
[2] Department of Physics, The University of Texas Rio Grande Valley, Brownsville, TX 78520, USA
[3] Department of Physics, University of California, Berkeley, CA 94720, USA
[4] Materials Sciences Division, Lawrence Berkeley National Laboratory, Berkeley, CA 94720, USA
[5] Contributed equally to this work

E-mail: xiang@berkeley.edu

Keywords: PT symmetry, acoustics, directional excitation

Abstract

We propose a mechanism for directional excitation without breaking reciprocity. This is achieved by embedding an impedance matched parity-time symmetric potential in a three-port system. The amplitude distribution within the gain and loss regions is strongly influenced by the direction of the incoming field. Consequently, the excitation of the third port is contingent on the direction of incidence while transmission in the main channel is immune. Our design improves the four-port directional coupler scheme, as there is no need to implement an anechoic termination to one of the ports.

Asymmetric wave transport is an important phenomenon in modern physics with a wide range of applications in various branches of physical science and Engineering. One application of asymmetric transport is directional excitation where the excitation of a third port depends on the direction of incoming field in the main channel. As depicted schematically in figure 1, one immediate approach to achieve directional excitation is via breaking reciprocity in the transmission line with an isolator.

Non-reciprocity has been achieved via the magnetic effect. In optics, the magnetooptical Faraday rotation is the basis of the Faraday isolator through which transmission of waves of selected polarization can be allowed or suppressed [1]. Moving frame induced by time dependent modulation resembles an effective magnetic feature and can be used as an alternative approach to obtain non-reciprocity. Asymmetric transport based on moving frame proposed in optics [2] and has been reported in opto-acoustics driven photonic crystal fiber [3], silicon chip [4], and acoustic ring cavity with circulating fluid inside [5]. In thermal transport, asymmetric wave propagation is proposed based on Coriolis force [6]. Nonlinear effects along with broken parity ($\mathcal{P}$) symmetry can lead to asymmetric transport [7–12]. Moreover, while nonlinear effects alone cannot produce asymmetric transport, a combination of nonlinear effect and judiciously balanced gain and loss elements, a signature of parity-time ($\mathcal{PT}$) symmetry systems, allow highly asymmetric transport [13–17]. However, directional excitation devices based on an embedded isolator (see figure 1(a)) will present severe limitations intrinsic to non-reciprocal schemes such as conversions of frequency, polarization or propagating mode, and restriction of coupling amplitude in flux conservative systems. Such drawbacks impede the integration of several of these elements on larger scale device as frequency or propagation mode will have to be modified multiple times during the operation.

The above issues lead us to the problem of a controllable directional excitation without breaking reciprocity. In this case, depicted schematically in figure 1(b), the upward port (third port) is only excited by input from the left-side while the transmission in the main channel remains unperturbed.

Recent progress in non-Hermitian physics indicate that linear parity-time ($\mathcal{PT}$) symmetric systems are good candidates to control wave propagation without breaking reciprocity. More specifically, phenomena such as unidirectional invisibility/transparency [18–20] and unidirectional lasing [21] are related to the asymmetric reflection in reciprocal $\mathcal{PT}$ systems and other phenomena such as loss induce transparency [22], reconfigurable

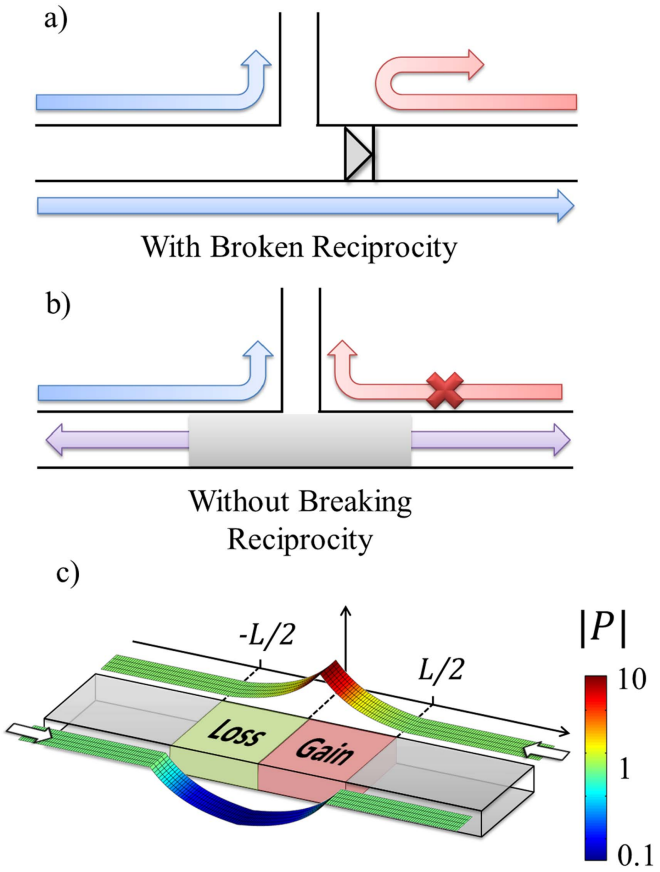

Figure 1. (a) Scheme of 3-port directional excitation with broken reciprocity, one isolator is inserted after the junction to provide directional excitation. As a consequence inputs from the right port are reflected. (b) Scheme of 3-port directional excitation without breaking reciprocity, excitation of third port depends on the direction of incidence but transmission in the main line is identical from both sides. (c) Asymmetric amplitude distribution in a waveguide with an impedance matched $\mathcal{PT}$ unit. Perfect transmission and zero reflection are observed for input form either sides. However, the field amplitude at the interface between loss and gain sections strongly depends on the input direction.

revivals [23], Brachistochrone wave dynamics [24] and lasing death (birth) [25–27] due to gain (loss) enhancement show that gain and loss parameter can be used as a knob to control field dynamics.

In this paper we propose a new method to overcome the aforementioned limitations of nonreciprocal schemes, and realize directional excitation *without* breaking reciprocity. More specifically, we show that by using $\mathcal{PT}$ symmetry and impedance matching one can obtain highly asymmetric coupling to the third port attached to the main channel. Unlike the directional excitation based on non-reciprocal elements, our method does not affect the forward and backward transmitted signal in the main channel. We stress that all linear structures including Non-Hermitian linear systems are reciprocal. However, the use of impedance matched $\mathcal{PT}$ symmetric arrangements provide an optimal and highly asymmetric behavior along with crucial properties required in the directional excitation scheme. Moreover, in contrast to previous devices, the amplitude coupled to the third channel can be designed independently from the transmission in the main channel. As a result, we demonstrate *super* directional excitation where the coupling to the third channel gets values larger than one. The impedance matching condition cancels spurious scattering event inside the active regions and ensures the $\mathcal{PT}$ element does not undergo any phase transition. Our proposed scheme provides a new approach for asymmetric wave transport in optics, electronics and acoustics, and might lead to design of a new type of compact directional couplers.

The physical mechanism for such a highly asymmetric field propagation relies on the cancellation of interference due to reflections at the loss and gain boundaries and sequential amplification and absorption in the gain and loss regions. Removing the reflections at the boundaries allows the field to penetrate the active region without generation of any net phase or amplitude[6]. During the propagation, as depicted in figure 1(c), the field amplifies (decays) first and then decays (amplifies) depending on the direction of excitation. Although transmission is unity for both incidences, one can observe that the field amplitude profile inside the active region

[6] In the case of complex valued impedance, the field can accumulate net gain/loss or phase when passing through an interface [37].

is highly asymmetric for the left and right excitations. At the interface between the gain and loss regions, the contrast between the two propagating fields is the largest. Interestingly, at the frequencies for which amplification and absorption are significant, highly asymmetric field amplitude in the transmission line reduces the possibility of interference between the forward and backward traveling fields, preventing the construction of standing waves around the contact area between gain and loss elements. This asymmetry in the right going and left going fields is used to perform directional excitation.

While our approach is applicable for general wave framework [28–30], we perform our analysis in acoustic wave propagation. To understand the basic principal behind such asymmetric excitation, it is beneficial to consider field propagation in a $\mathcal{PT}$ symmetric impedance matched 1D acoustic waveguide where the acoustic waves $Pe^{i\omega t}$ are propagating in the z direction. The pressure field propagation can be described by the Helmholtz equation [31]

$$\frac{d^2}{dz^2}P(z) + \omega^2\rho(z)\kappa(z)^{-1}P(z) = 0. \tag{1}$$

In equation (1), $P(z)$ is the acoustic pressure (deviation from the atmospheric pressure) along the direction of propagation z, $\omega = 2\pi f$ (f is the frequency) the so-called angular frequency, ρ is the static mass density of the medium, and κ its bulk modulus. As depicted in figure 1, for a normal incident field, the $\mathcal{PT}$ symmetric impedance matched waveguide satisfies (i) symmetric relations $\kappa(z) = \kappa^*(-z)$, $\rho(z) = \rho^*(-z)$ and (ii) impedance matching condition $Z_i = Z_0$, where $Z_i = \sqrt{\rho_i\kappa_i}$ is the impedance of the medium i. In our numerical simulation we assumed that outside of the active region, namely $|z| > L/2$, the waveguide is filled by air with real parameters $\kappa_0 = 1.47 \times e^5$ Pa and $\rho_0 = 1.25\,\mathrm{kg\,m^{-3}}$. The $\mathcal{PT}$ cell is composed of loss and gain medium with $\kappa_{1,2} = \frac{\kappa_0}{a}\exp(\pm i\theta)$ and $\rho_{1,2} = \rho_0 a\exp(\mp i\theta)$ in regions $-L/2 \leqslant z \leqslant 0$ and $0 \leqslant z \leqslant L/2$, respectively.

Generally the effective density (modulus) of acoustic material should have a negative (positive) imaginary part, indicating the material is lossy with inherent damping. The acoustic gain material has not yet been observed in nature, which however can be effectively realized by delicate feed-back systems using the active sound controlling apparatus [12, 30, 32, 33].

Outside the active regions the Helmholtz equation admits solutions $P_L = P_L^+e^{-ikz} + P_L^-e^{ikz}$ for $z \leqslant -L/2$ and $P_R = P_R^+e^{-ikz} + P_R^-e^{ikz}$ for $z \geqslant L/2$, where k is the wave number, and $P^{+(-)}$ is the amplitude of the forward (backward) traveling acoustic waves. The forward and backward components on left and right of the active layers are connected through the 2×2 transfer matrix M

$$\begin{pmatrix} P_R^+ \\ P_R^- \end{pmatrix} = M\begin{pmatrix} P_L^+ \\ P_L^- \end{pmatrix}, \quad M(k) = \begin{pmatrix} m_{11} & m_{12} \\ m_{21} & m_{22} \end{pmatrix}. \tag{2}$$

Elements of the transfer matrix are directly related to the left-to-right (right-to-left) transmission, $t_L \equiv \frac{P_R^+}{P_L^+}$ $\left(t_R \equiv \frac{P_L^-}{P_R^-}\right)$, and left (right) reflection, $r_L \equiv \frac{P_L^-}{P_L^+}$ $\left(r_R \equiv \frac{P_R^+}{P_R^-}\right)$, amplitudes:

$$t_L = \frac{1}{m_{22}},\ r_L = -\frac{m_{21}}{m_{22}},\ t_R = \frac{1}{m_{22}},\ r_L = \frac{m_{12}}{m_{22}}. \tag{3}$$

For our 1D $\mathcal{PT}$ system depicted in figure 1(c) the transfer matrix is given by

$$M = D_{0,-L/2}^{-1}K_{2,0}D_{2,L/2}K_{1,2}D_{1,L/2}K_{0,1}D_{0,-L/2}. \tag{4}$$

Above

$$K_{i,j} = \frac{1}{2}\left(1 + \frac{Z_j}{Z_i}\right)\mathbf{I} + \frac{1}{2}\left(1 - \frac{Z_j}{Z_i}\right)\boldsymbol{\sigma}_x \tag{5}$$

and

$$D_{j,z} = \cos\left(k\sqrt{\frac{\rho_j\kappa_0}{\kappa_j\rho_0}}z\right)\mathbf{I} + i\sin\left(k\sqrt{\frac{\rho_j\kappa_0}{\kappa_j\rho_0}}z\right)\boldsymbol{\sigma}_z \tag{6}$$

where $\mathbf{I}$ is a 2×2 unit matrix and $\boldsymbol{\sigma}_{x,z}$ are the corresponding Pauli matrices. K is the kick matrix, which connect boundaries between the different media (impedance matrix). The D matrix is the phase matrix, which provides the phase generated by propagation in the medium. Using the equations (5), (6) and the aforementioned mass density and bulk modulus, it is easy to show that $K_{1,2} = K_{0,1} = K_{2,0} = \mathbf{I}$. Consequently transfer matrix $M = D_{2,L/2}D_{1,L/2}$ would given by

$$M = \cos(kLa\cos\theta)\mathbf{I} + i\sin(kLa\cos\theta)\boldsymbol{\sigma}_z. \tag{7}$$

As a result the transfer matrix is a diagonal matrix where its non-zero elements correspond to a phase. Hence, a wave traveling in this impedance matched $\mathcal{PT}$ cell will not be affected by any reflection and will acquired a phase given by $kLa\cos\theta$. However, the dynamics inside each individual active layer is quite different. In the gain layer

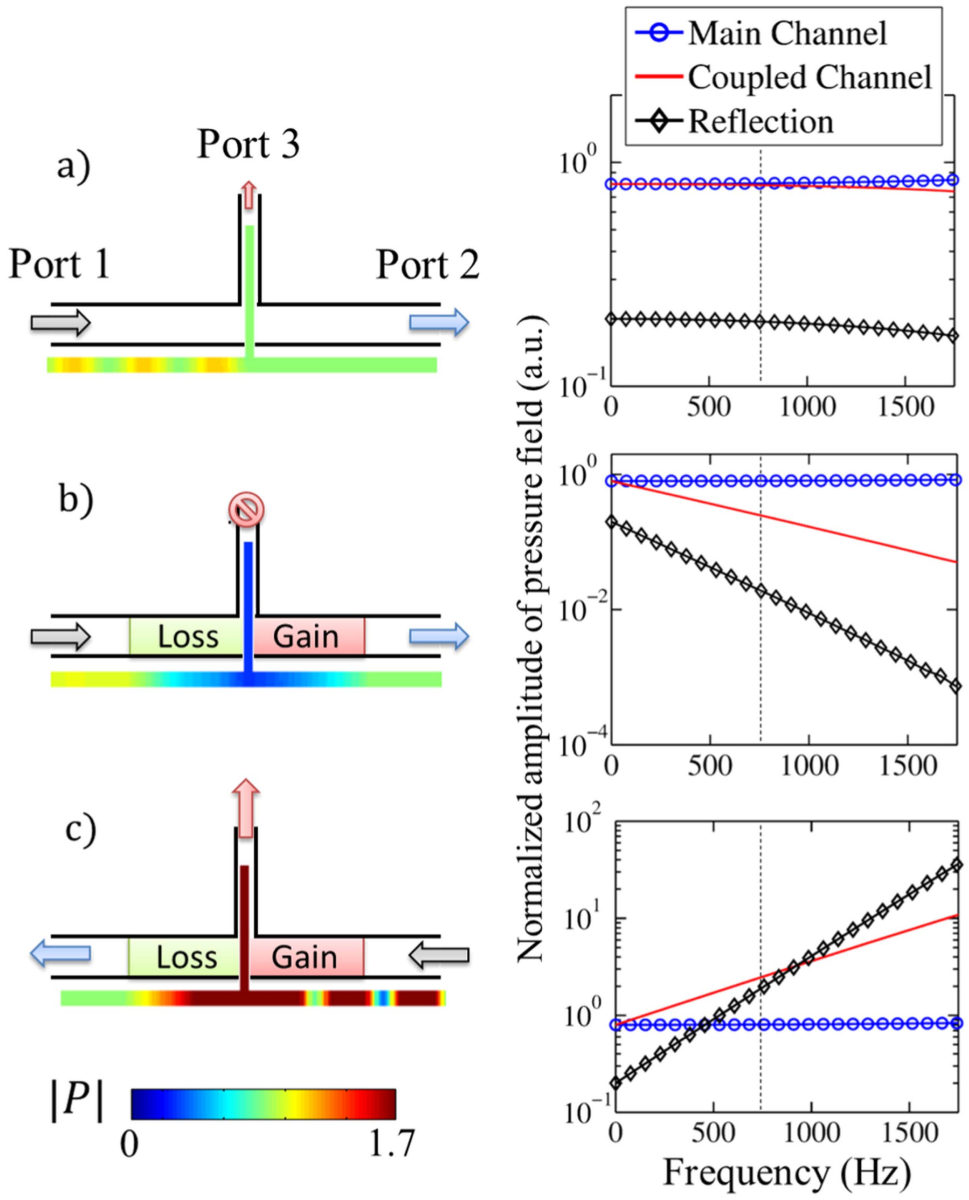

Figure 2. (a) Scheme of the empty three port waveguide, the amplitude of the pressure field distribution incident from port 1 is superimposed. (b) and (c) Same three port waveguide with the impedance matched $\mathcal{PT}$ unit inserted and pressure field input from the left (loss side) and right (gain side), respectively. In the right panels, transmission in the main channel (circle blue), coupling to port 3 (solid red) and reflection (diamond black) as functions of frequency are presented for the corresponding cases. All amplitudes are normalized to the input. (b) When excited from the left side, the coupling to the third port is inhibited. (c) Excitation of the third port is observed when the field is incident from the gain side. This asymmetric behavior between left and right inputs validates our directional excitation scheme. Moreover, the transmission in the main channel (circle blue) is identical in the three cases, as reciprocity is not broken by the $\mathcal{PT}$ cell.

the field accumulates an amplification equal to $\alpha = \exp\left(k\frac{L}{2}a\sin\theta\right)$ while in the loss layer it decays by the inverse amount.

These analytical results are in agreement with numerical simulations using finite element solver (Comsol Multiphysics). Figure 1(c) presents the amplitude of the pressure field for left and right going waves propagating in a 1D waveguide containing the impedance matched $\mathcal{PT}$ cell. The corresponding parameters for the gain and loss regions are given by $\rho_{1,2} = \rho_0 a e^{i\theta_{1,2}}$ and $\kappa_{1,2} = \frac{\kappa_0}{a}e^{-i\theta_{1,2}}$ with $a = 1.022$ and $\theta_{1,2} = \pm 0.21$ rad. The length of the gain and loss cell is $L/2 = 0.4$ m. For these parameters, the calculated maximum amplification (attenuation) ratio is $\alpha = 10.4$ $(1/\alpha = 0.096)$ which agrees with numerical simulations.

The highly asymmetric field amplitude at the interface of the gain and loss layers helps us to control the amplitude of the signal transmitted to the third channel and generate asymmetric excitation. Figure 2(a) presents a scheme of our numerical demonstration, a 6 cm wide waveguide sets the main channel between port 1 and port 2. A secondary waveguide with half width (3 cm) is perpendicularly connected to the main channel. Figure 2(a)

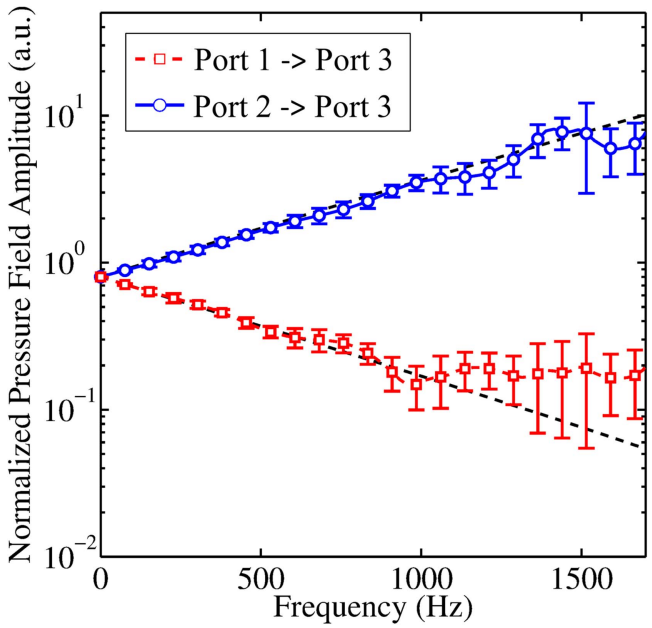

Figure 3. Amplitude coupled to the third port in presence of perturbations in the acoustic parameters of the $\mathcal{PT}$ unit. Red square dashed line shows the drop of the coupled amplitude when excited from the loss side and blue circled solid line when excited from the gain side. These curves are obtained after averaging coupled amplitude over ten different simulations with 10% random deviation on real and imaginary part of both loss and gain medium. Because of this perturbation, the system slightly deviates from impedance matching and $\mathcal{PT}$ symmetric condition. The two dotted black lines represent the perfect case scenario obtained without perturbation.

also shows the amplitude of the pressure field in this passive 3-port waveguide at frequency 750 Hz. The right panel presents the amplitude of the transmission in the main channel (blue line ∘), the transmission to the coupled port (red line) and the reflection (black line ◊) as a function of the frequency. These features are moderately dispersive as the main and side waveguides are sub-wavelength ($\lambda_{1500\text{Hz}} = 22.9$ cm). The passive 3-port waveguide is spatially symmetric such as forward propagation (incident from port 1) and backward propagation (incident from port 2) give the same results.

The transmission to port 3 linearly depends on the local amplitude of the pressure field at the contact point. In figures 2(b)–(c), the impedance matched $\mathcal{PT}$ unit is inserted in the center of the main channel such as the interface between loss and gain medium is exactly below the contact point of the side waveguide. In this case, the amplitude of the signal measured at port 3 depends on the direction of propagation inside the main channel. When incident from port 1, the pressure field has to travel through the loss medium first resulting in a reduced amplitude at the interface and a significantly reduced coupling to the side channel. On the contrary, the incidence from port 2 leads to the amplification of the pressure field at the interface and the increase of the transmission to port 3 which for most of the frequencies is larger than unity. The right panels in figures 2(b)–(c) present the reduction and amplification of the transmission to port 3 obtained for each incidence in the function of frequency. A contrast of $C = \frac{t_{1,3} - t_{2,3}}{t_{1,3} + t_{2,3}} \approx 98\%$ between the two incidences is already achieved at 1500 Hz frequency where $t_{I,O}$ is the transmitted signal from port I to port O. Furthermore, one can observe that the transmission in the main channel is independent from the incidence and not affected by the $\mathcal{PT}$ unit. Accordingly, the amplitude of the reflections will vary in order to satisfy the pseudo energy conservation relation. The aforementioned transmission property is specific to the $\mathcal{PT}$ symmetric systems and allows us to maintain the transmission of the information in the main channel. This is in contrast to previous proposals based on isolators where one alters the carrier frequency, the propagating mode or spoils the transmission in the main channel [2, 5, 10].

In above discussions, we consider that the acoustic parameters of the loss and gain regions satisfy $\mathcal{PT}$ symmetry and impedance matching condition. However, these requirements could be difficult to meet perfectly in experimental demonstration. Our numerical study shows that the directional excitation is achievable even with perturbed acoustic parameters. A deviation of 10% magnitude is randomly generated and affects both the modulus and argument of the acoustic parameters. Figure 3 presents the transmission to port 3 for both incidence averaged over ten perturbed scenario. The black dash lines represent the perfect cases extracted from figures 2(b)–(c) while the red and blue are the perturbed cases with incidence from port 1 and port 2, respectively. For higher frequencies, wavelength becomes comparable to the size of gain and loss region.

Therefore, the scattering at the interfaces becomes dominant and causes a bigger deviation from the perfect case. However, the average contrast observed is maintained at 90% $\pm$ 10% for frequencies higher than 1000 Hz.

Finally we would like to mention the experimental feasibility of our proposal. Recent development in active acoustic metamaterials indicates that one can achieve a broad range of effective parameters [34]. Furthermore, digital electronics enables arbitrary and real-time control of metamaterial acoustic and elastic properties [32, 33, 35, 36].

In conclusion, we have shown that using $\mathcal{PT}$ symmetric impedance matched layered media one can achieve highly directional excitation without breaking reciprocity. In a three port acoustic system the acoustic pressure can be detected in the third port only when it emitted from gain side. The transmission in the main waveguide remain reciprocal and is the same as the passive three port system. Our proposal might has a vast range of application in different branches of physics.

Acknowledgments

This work was funded by the Director, Office of Science, Office of Basic Energy Sciences, Materials Sciences and Engineering Division, of the U.S. Department of Energy under Contract No. DE-AC02-05-CH11231.

References

[1] Saleh B E A and Teich M C 1991 *Fundamentals of Photonics* (New York: Wiley)
[2] Yu Z and Fan S 2008 *Nat. Phot.* **3** 91
[3] Kang M S, Butsch A and Russell P S J 2011 *Nat. Phot.* **5** 549
[4] Lira H, Yu Z, Fan S and Lipson M 2012 *Phys. Rev. Lett.* **109** 033901
[5] Fleury R, Sounas D L, Sieck C F, Haberman M R and Alu A 2014 *Science* **343** 516
[6] Li H and Kottos T 2015 *Phys. Rev.* E **91** 020101(R)
[7] Konotop V V and Kuzmiak V 2002 *Phys. Rev.* B **66** 235208
[8] Lepri S and Casati G 2011 *Phys. Rev. Lett.* **106** 164101
[9] Fan L, Wang J, Varghese L T, Shen H, Niu B, Xuan Y, Weiner A M and Qi M 2012 *Science* **335** 447
[10] Liang B, Guo X S, Tu J, Zhang D and Cheng J C 2010 *Nat. Mater.* **9** 989
[11] Boechler N, Theocharis G and Daraio C 2011 *Nat. Mater.* **10** 665
[12] Popa B I and Cummer S A 2014 *Nat. Commun.* **5** 3398
[13] Ramezani H, Kottos T, El-Ganainy R and Christodoulides D N 2010 *Phys. Rev.* A **82** 04380
[14] Bender N, Factor S, Bodyfelt J D, Ramezani H, Christodoulides D N, Ellis F M and Kottos T 2013 *Phys. Rev. Lett.* **110** 234101
[15] Peng B, Ozdemir S K, Lei F, Monifi F, Gianfreda M, Long G L, Fan S, Nori F, Bender C M and Yang L 2014 *Nat. Phys.* **10** 394
[16] Chang L, Jiang X, Hua S, Yang C, Wen J, Jiang L, Li G, Wang G and Xiao M 2014 *Nat. Phot.* **8** 524
[17] Nazari F, Bender N, Ramezani H, Moravvej-Farshi M K, Christodoulides D N and Kottos T 2014 *Opt. Exp.* **22** 9574–84
[18] Lin Z, Ramezani H, Eichelkraut T, Kottos T, Cao H and Christodoulides D N 2011 *Phys. Rev. Lett.* **106** 213901
[19] Regensburger A, Bersch C, Miri M A, Onishchukov G, Christodoulides D N and Peschel U 2012 *Nature* **488** 167
[20] Zhu X, Feng L, Zhang P, Yin X and Zhang X 2013 *Opt. Lett.* **38** 2821
[21] Ramezani H, Li H, Wang Y and Zhang X 2014 *Phys. Rev. Lett.* **113** 263905
[22] Guo A *et al* 2009 *Phys. Rev. Lett.* **103** 093902
[23] Ramezani H, Christodoulides D N, Kovanis V, Vitebskiy I and Kottos T 2012 *Phys. Rev. Lett.* **109** 033902
[24] Ramezani H, Schindler J, Ellis F M, Günther U and Kottos T 2012 *Phys. Rev.* A **85** 062122
[25] Chitsazi M, Factor S, Schindler J, Ramezani H, Ellis F M and Kottos T 2014 *Phys. Rev.* A **89** 043842
[26] Brandstetter M, Liertzer M, Deutsch C, Klang P, Schoberl J, Tureci H E, Strasser G, Unterrainer K and Rotter S 2014 *Nat. Comm.* **5** 4034
[27] Peng B, Ozdemir S K, Rotter S, Yilmaz H, Liertzer M, Monifi F, Bender C M, Nori F and Yang L 2014 *Science* **346** 328–32
[28] Makris K G, El-Ganainy R, Christodoulides D N and Musslimani Z H 2008 *Phys. Rev. Lett.* **100** 103904
[29] Schindler J, Li A, Zheng M C, Ellis F M and Kottos T 2011 *Phys. Rev.* A **84** 040101(R)
[30] Zhu X, Ramezani H, Shi C, Zhu J and Zhang X 2014 *Phys. Rev.* X **4** 031042
[31] Morse P M 1948 *Vibration and Sound* 2nd edn (New York: McGraw-Hill)
[32] Fleury R, Sounas D L and Alu A 2014 *Nat. Comm.* **6** 5905
[33] Shi C, Dubois M, Chen Y, Cheng L, Ramezani H, Wang Y and Zhang X 2016 *Nat. Comm.* **7** 11110
[34] Popa B, Zigoneanu L and Cummer S A 2013 *Phys. Rev.* B **88** 024303
[35] Popa B, Shinde D, Konneker A and Cummer S A 2015 *Phys. Rev.* B **91** 220303(R)
[36] Christensen J, Willatzen M, Velasco V R and Lu M- H 2016 *Phys. Rev. Lett.* **116** 207601
[37] Basiri A, Vitebskiy I and Kottos T 2015 *Phys. Rev.* A **91** 063843